PLLaVA : Parameter-free LLaVA Extension from Images to Videos for Video Dense Captioning

Lin Xu[1*], Yilin Zhao[2*], Daquan Zhou[3⋆†], Zhijie Lin[3], See Kiong Ng[1], Jiashi Feng[3]

[1]National University of Singapore [2]New York University [3]Bytedance

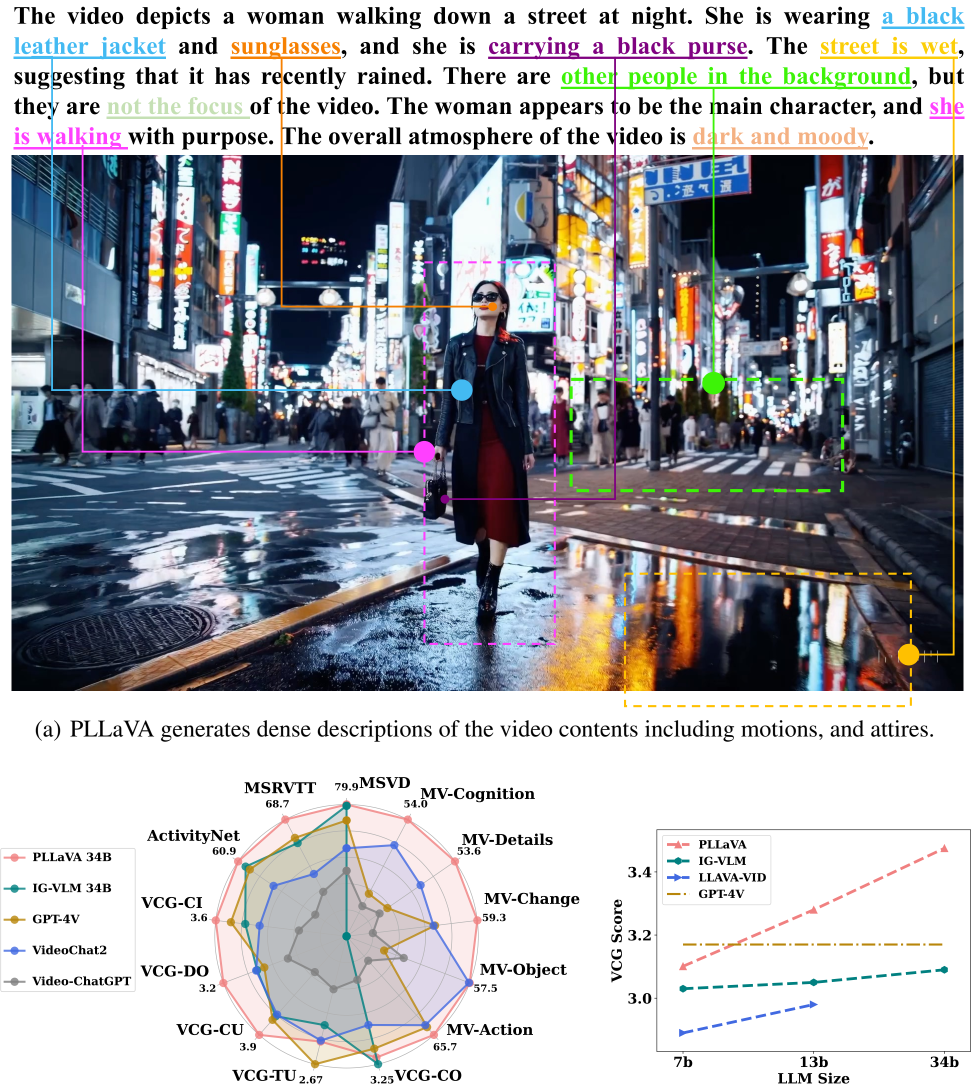

The video depicts a woman walking down a street at night. She is wearing a black leather jacket and sunglasses, and she is carrying a black purse. The street is wet, suggesting that it has recently rained. There are other people in the background, but they are not the focus of the video. The woman appears to be the main character, and she is walking with purpose. The overall atmosphere of the video is dark and moody.

(a) PLLaVA generates dense descriptions of the video contents including motions, and attires.

(b) State-Of-The-Arts on various video understanding tasks. (c) Better model scaling performance.

Figure 1: Performance presentation of PLLaVA . (a) An example of captions generated with PLLaVA 34B. (b) Performance comparison of PLLaVA with recent strong baselines over different video benchmarks and (c) the scaling curve of PLLaVA and recent SOTA methods.

[*] Equal contribution. [⋆]Project lead. [†]Corresponding authors. Lin Xu, cathyxl2016@gmail.com; Daquan Zhou, zhoudaquan21@gmail.com

Preprint. Under review.

Abstract

Vision-language pre-training has significantly elevated performance across a wide range of image-language applications. Yet, the pre-training process for video-related tasks demands exceptionally large computational and data resources, which hinders the progress of video-language models. This paper investigates a straightforward, highly efficient, and resource-light approach to adapting an existing image-language pre-trained model for dense video understanding. Our preliminary experiments reveal that directly fine-tuning pre-trained image-language models with multiple frames as inputs on video datasets leads to performance saturation or even a drop. Our further investigation reveals that it is largely attributed to the bias of learned high-norm visual features. Motivated by this finding, we propose a simple but effective pooling strategy to smooth the feature distribution along the temporal dimension and thus reduce the dominant impacts from the extreme features. The new model is termed Pooling LLaVA, or PLLaVA in short. PLLaVA achieves new state-of-the-art performance on modern benchmark datasets for both video question-answer and captioning tasks. Notably, on the recent popular Video ChatGPT benchmark, PLLaVA achieves a score of 3.48 out of 5 on average of five evaluated dimensions, exceeding the previous SOTA results from GPT4V (IG-VLM) by 9%. On the latest multi-choice benchmark MVBench, PLLaVA achieves 58.1% accuracy on average across 20 sub-tasks, 14.5% higher than GPT4V (IG-VLM). Code is available at https://github.com/magic-research/PLLaVA.

1 Introduction

Multimodal Large Language Models (MLLMs) have demonstrated remarkable proficiency in image comprehension when trained on large-scale image-text pairs [16, 48, 26, 24, 11]. Analogous to the image domain, the recent video understanding models also explore a similar pipeline to fine-tune LLMs on large-scale video-text data [3, 17, 18]. However, this method suffers a high cost of computing resources and video data annotations. A more pragmatic approach is to *adapt* the pre-trained image-domain MLLMs to video data [30, 27, 14].

An intuitive method for image MLLM adaption is to encode multiple video frames into a sequence of features and directly feed them into MLLMs, as the Large language Models(LLMs) [36, 35] are native for processing sequential features and shown to be capable of understanding temporal information [21, 28]. However, we empirically found two technical challenges when extending image MLLMs to video data in this way. First, compared to zero-shot applications, training the image MLLM on video data does not always increase the performance but introduces performance vulnerability to the change of inquiry prompts. Secondly, increasing the size of the language model component does not improve the video understanding performance. Those two observations are counter-intuitive since scaling up model sizes and exposing models to more downstream data are typically considered beneficial for model performance.

We then conducted a series of studies to investigate the root cause of these two observations. For the first one, we found it is mainly due to the limited information encoded by the image encoder. When experimenting on LLaVA [26] with 4-frame inputs, we experimentally found that, as shown in Figure 3, some visual feature tokens have dominantly larger norms over the others during the fine-tuning process. These tokens lead to shorter text descriptions with lower quality. As demonstrated in Figure 2, the 4-frame models tend to generate shorter texts with training on more samples. We conjecture that the large-norm features have obtained global video information and thus suppress the norms of other tokens, due to the softmax calculation during the self-attention. This leads the generated description to be short. Even worse, if the prompt template changes, the learned MLLMs would completely collapse, leading to rather short descriptions or even no response. We observe that adding more video frames could mitigate the suppression of the majority of the tokens. However, this would lead to significantly larger memory consumption.

Thus, there is a trade-off between the number of frames and the computation cost. The intuitive way is to downsample the video frames. However, directly averaging the spatial and temporal dimensions as has been done in VideoChatGPT [30] loses too much spatial information and also does not achieve optimal performance during the scaling of the training dataset. Thus, the target is to find the minimum

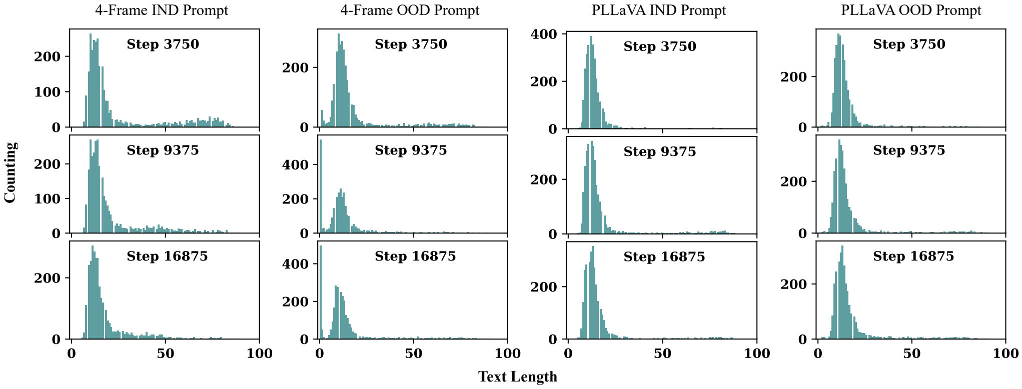

Figure 2: Histograms of generation text length distribution for 4-Frame and PLLaVA . x-axis are text lengths, y-axis indicates the counting of text-lengths. 4-Frame generates shorter texts under more training steps and the out-of-distribution prompt, while PLLaVA remains consistent in both situations.

spatial resolution of each frame that does not degrade the scaling curve. To achieve this, we adopt a pooling [15] operation to explore the optimal settings such that it does not degrade the benefits of increasing the temporal receptive field. The impact of the pooling operation is shown in Figure 7.

For the second observed phenomenon, we believe one main reason is the poor quality of the video dataset, compared to the image dataset. Specifically, many of the video datasets are in question-answer formats and the descriptions of the videos might be short. Thus, as the model learns the temporal description from the video dataset, the description of other metrics such as the objects and the spatial relations degrades. the stronger the LLM is, the faster the output degrades. Instead of building high-quality video datasets, we choose to explore architectural and optimization algorithms to better preserve the learned information in image datasets during the learning of the temporal information on video datasets. To achieve this, we utilize the tricks of weight fusion. We set two groups of weights: one from the image pre-raining and one with video dataset fine-tuning. After training, we searched to find the optimal combination of the image-based model weights and the video-based model weights in the hope that the combined model could gather benefits from both datasets. The process is termed post-training optimization in this paper and its impacts are shown in Figure 5.

- We performed a thorough initial investigation for directly applying image large multi-modality models to video tasks and found several failure modes. We then introduce an elegantly simple yet highly potent pooling strategy that systematically achieves the optimal balance between training efficiency and caption accuracy.
- We introduce a post-training model merging method that could effectively reduce the forgetting phenomenon of the large language models during multi-modality fine-tuning. With this, we are able to get a large video multi-modality model with 34B LLMs without the extra creation of high-quality datasets.
- We conduct extensive experiments to verify the superiority of the proposed model and achieve a new state-of-the-art across various video understanding benchmarks, especially for video captioning tasks with dense captions. With Pool-LLaVA, we do the re-captioning of the top 1M video data from Panda-70M with highly dense and accurate bilingual captions.

2 Related Works

Video Multimodal Large Language Models Video Multi-modality Models process video input and generate responses according to user commands. Commonly, they incorporate a projection network [30, 22, 19], inter-modality attention [17, 18] or a modality perceiver [45, 32, 12] as learnable interfaces. These interfaces are instrumental in melding the spatial-temporal dynamics of videos with large language models' (LLMs) processing capabilities, by transforming video content into a sequence of tokens that LLMs can adeptly analyze. BLIP [16] marked a significant milestone by integrating a frozen vision encoder with BLIP to enhance video processing efficiency, with only the newly added Q-Former learnable. Demonstrating remarkable zero-shot capabilities in Video Question Answering (VQA), it outperformed existing techniques of its time. Extending the innovations of its predecessors, Video-ChatGPT [30] introduced the trailblazing approach of video instruction tuning, along with creating a dataset of high-quality instructional data. This initiative set a new standard for assessing models through video-based text generation benchmarks. VideoChat [17] employed cross-attention mechanisms to skillfully condense video tokens, aligning user queries with the dialogue context to enhance the model's interpretative capabilities. Building upon these advances, VideoChat2 [18] refined the approach with a multi-stage bootstrapping technique that honed in on modality alignment and instruction tuning, amassing a robust collection of high-quality video data for fine-tuning instruction-driven tasks. VILA [23] proposes more advanced training recipes. Further integrating modalities, Video-LLaVA [22] leveraged a pre-aligned encoder adaptable to both images and videos, facilitating shared projections and enabling synergistic training across image and video-related tasks. CAT [41] introduces both video and audio to futher enhance understanding.

Long videos present significant challenges due to their intrinsic high computational complexity and extensive memory requirements. Handling the entire span of a long video with video tokens poses difficulties in jointly capturing spatial details and temporal dynamics effectively. In response, Video Language Models (Video MLLMs) have adopted sophisticated temporal modeling techniques to address these challenges with greater efficiency. MovieChat [32] implemented a novel memory-based mechanism within transformers, strategically combining similar frames to reduce both computational load and memory footprint. Chat-UniVi [12] debuted a harmonized approach for processing images and videos, innovatively condensing spatial and temporal tokens through dynamic token merging, utilizing k-NN algorithms for improved efficiency. LLaMA-VID [19] innovated with a dual-token approach that effectively condensed video representations by segregating context and content tokens, allowing for more efficient compression. VTimeLLM [10] emphasize the boundaries of videos by introducing a new question answering dataset. Advancing this innovation, Vista-LLaMA [29] introduced EDVT-Attention along with a sequential vision projector that meticulously curates visual tokens and condenses temporal tokens, progressively amalgamating them with a Q-former mechanism. To further optimize the handling of extended videos, certain models emphasized the selective processing of keyframes, thus diminishing the volume of video frames required and streamlining the overall computational demands.

Pipelined Video Understanding Capitalizing on the Video MLLM framework, a novel approach emerged involving the use of pre-existing Video Models coupled with LLMs through a multi-stage process of video modality conversion. This method entails translating video content into textual narratives, typically through the employment of pretrained VideoLMs, before integrating with an LLM in the final phase. By encapsulating videos as text tokens, it leverages the LLMs' adeptness at navigating textual data, thereby permitting the interpretation of temporal sequences via these crafted descriptions. VideoChat-Text [17] adeptly converts video streams into comprehensive text descriptions, encapsulating a range of video elements. Meanwhile, LLoVi [44] unveiled an efficient, LLM-centric framework tailored for addressing queries that span long video durations. Here, video captioning agents transcribe videos into detailed textual descriptions which the LLMs then distill to enhance long-duration video comprehension. While the aforementioned methodologies primarily translate video into text for LLM processing, LLMs are concurrently being explored for their capacity to facilitate video analysis through program generation. ViperGPT [34] is a pioneering example, harnessing code-producing LLMs, including the likes of GPT-3 Codex [4]. It effectively utilizes a visual module API catering to text-based queries and crafts programs that scrutinize image or video content, furnishing informed responses to those queries. Similarly, ProViQ [5] engages an LLM to craft Python scripts that enact multi-stage procedural reasoning in the context of zero-shot video queries, processing these scripts to ascertain solutions to posed questions.

3 Method & Analysis

Adapting image MLLMs into the video domain can be tricky and vulnerable to the designs of model structures. In this section, we first present some challenges encountered when extending image MLLMs to video, drawing insights from our comprehensive experiments and analyses. Corresponding solutions to these challenges will be presented, forming the integral framework of PLLaVA .

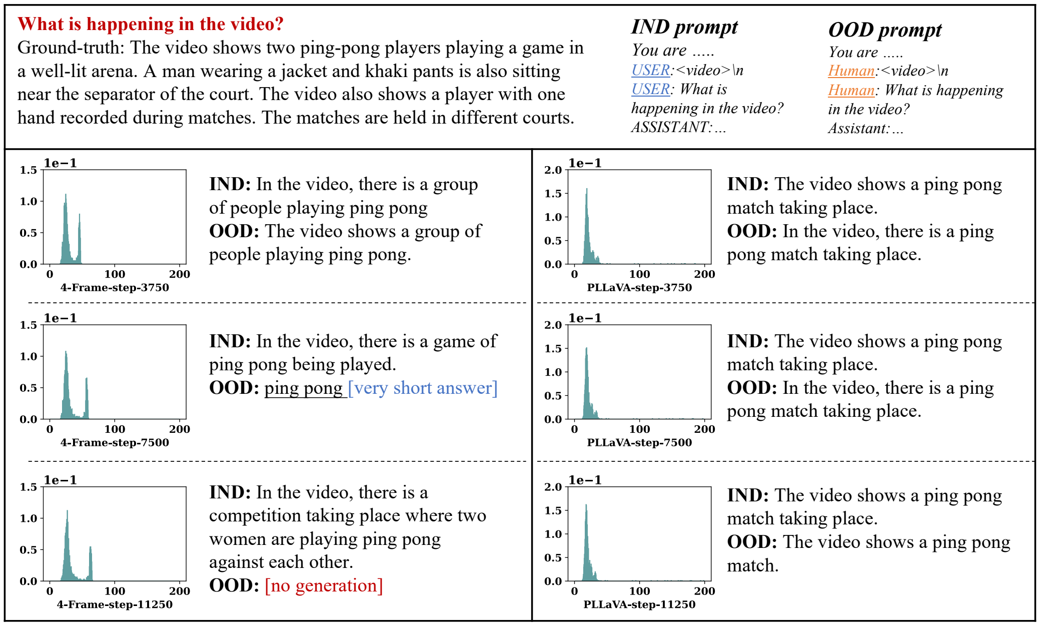

What is happening in the video?

Ground-truth: The video shows two ping-pong players playing a game in a well-lit arena. A man wearing a jacket and khaki pants is also sitting near the separator of the court. The video also shows a player with one hand recorded during matches. The matches are held in different courts.

IND prompt

You are .....
USER:<video>\n
USER: What is happening in the video?
ASSISTANT:...

OOD prompt

You are .....
Human:<video>\n
Human: What is happening in the video?
Assistant:...

IND: In the video, there is a group of people playing ping pong
OOD: The video shows a group of people playing ping pong.

IND: The video shows a ping pong match taking place.
OOD: In the video, there is a ping pong match taking place.

IND: In the video, there is a game of ping pong being played.
OOD: ping pong [very short answer]

IND: The video shows a ping pong match taking place.
OOD: In the video, there is a ping pong match taking place.

IND: In the video, there is a competition taking place where two women are playing ping pong against each other.
OOD: [no generation]

IND: The video shows a ping pong match taking place.
OOD: The video shows a ping pong match.

Figure 3: A example comparing the norm distributions and generated texts of the *n-frame* and our PLLaVA . From top to down, dominant tokens(with high norms) appear and increase as more data sample trained under the *n-frame* setting, which is accompanied by a decline in generation quality, especially under the out-of-distribution prompt. On the right column, our PLLaVA 's norm distributions are consistent as well as the generated texts under various number of training data and prompts.

3.1 Failure Cases Analysis for Applying Image MLLMs

We first explored a direct way to adapt image MLLMs into the video domain: encoding selected video frames with image encoders separately and concatenating these frame features as input to the image MLLMs. This is to utilize the capability of LLMs to interpret the temporal information in the encoded video frames. We coined this method as *n-frame*. Specifically, given a sequence of video frames $\mathbf{X} \in \mathbb{R}^{T \times C \times W \times H}$, we obtain the features for each frame via the vision encoder pre-trained in CLIP-ViT [31] models and the encoded frames features are represented as $X_v \in \mathbb{R}^{T \times w \times h \times d}$. The *n-frame* method is formulated as:

$$r = \text{MLLM}(X_v, X_t), \tag{1}$$

where X_t is the text inputs and r is the output texts. Nonetheless, during our efforts to train the MLLM in this scenario, we encountered two issues that hindered us from achieving optimally performance models.

Vulnerability to prompts. The first observation is that the models trained with *n-frame* could be highly sensitive to prompt patterns when dealing with generation tasks. Figure 3 illustrates such a phenomenon. We divide the prompts into two categories: in-distribution (IND) and Out-of-Distribution (OOD). In the left part of the figure, when generating under the prompt pattern used in training (IND), the model can generate decent descriptions about the video despite its tendency of shorter generation length with more data samples trained. However, if we prompted the model with OOD prompts, in which we just changed the tags for the two roles in a conversation, the quality of the generated response then drastically declined. The generation has content in normal length under the model trained for 3750 steps. However, for the longer trained models, the generations are shorter for 7500 steps, and even no response for 11250 steps. This example demonstrate the vulnerability of the *n-frame* method.

Dominant tokens. In view of the vulnerability of *n-frame* models stated above, we proceeded to analyze the variance between models at their initial stages of training and when fully trained. By visualizing the norm of vision tokens across models trained at different stages, we observed a trend

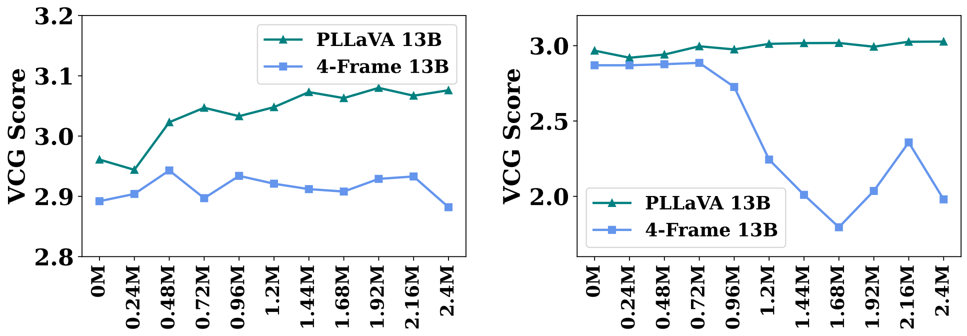

(a) IND prompt.

(b) OOD prompt.

Figure 4: When training with more samples, (a) and (b) show performance of *n-frame* method is stagnant while pooling can keep rising. Curves in (b) indicate the vulnerability of *n-frame* to prompt design while pooling is more robust.

towards the emergence of dominant tokens(with high norms) as training samples increased, as shown by the histograms in Figure 3. Furthermore, the twin-tower distribution is much wider when trained with more data. Therefore, we speculate there exists a plausible correlation between these dominant tokens and the degradation of generation under OOD prompt. The distribution comparisons between *n-frame* and the proposed PLLaVA can further validate the conjecture, which is explained in Sec. 4.4.

Data scaling failures. Based on the aforementioned phenomena, it can be inferred that employing image MMLMs to video and seeking to benefit from the scaling of video data samples can pose a challenging issue. We present the performance curve of *n-frame* method under different training samples in Figure 4. The blue curve representing performance tendency of *n-frame* keeps stagnant under IND prompt, and degrades a lot under OOD prompts after the training sample exceeds 0.48M. Similar patterns are observed in the experimental findings of Video-ChatGPT [30], as detailed in Table 1. Video-ChatGPT [30] introduces a unique pooling strategy that involves averaging visual features across the temporal dimension as well as the spatial dimension, resulting a visual feature $X_{vcg} \in \mathbb{R}^{(T+w\times h)\times d}$ after concatenating both dimensions. This feature is then fed into LLMs to generate corresponding response. The first two columns of Table 1 demonstrate our replication of Video-ChatGPT using their 100K video-text dataset, while the third column illustrates a significant deterioration in model performance upon introducing additional training video data samples from VideoChat2 [18]. Consequently, the identification of effective strategies for models to harness the growing volume of data remains a critical issue.

Method	Video-ChatGPT		
	reported	reproduce	scaled
Dataset	100K	100K	100K+249K
VCG Score	2.38	2.41	1.94

Table 1: Video-ChatGPT [30] fails in data scaling.

3.2 Model Scaling Degradation

Our investigation on current video models reveals that increasing the model size does not typically result in significant improvements in performance for most models. We draw the performance of a recent work IG-VLM [14] and our attempts in Figure 5. IG-VLM achieves almost no difference when applying 7B, 13B, and 34B models of LLaVA-Next [25]. In our attempts of with pooling features (the first column of Figure 5), the performance of LLaVA-Next 34B is even worse than its 13B LLaVA-Next model. For IG-VLM, the input video frames are combined to a grid view image, confined by the resolution, leading to the unsatisfactory scaling ability. As for our attempts, we found a tendency of shorter generations

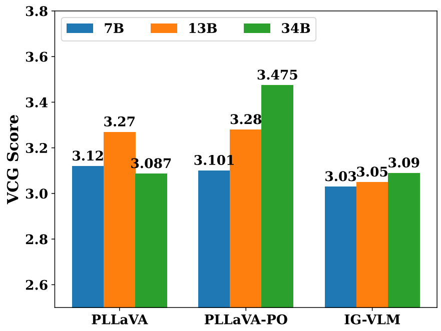

Figure 5: Video MLLMs fail to improve when scaling model size. Post Optimization resolves the scaling degradation.

with larger MLLMs, thus we owe the degradation to the quality of video-text data pairs, which undermines the generation ability of LLMs in MLLM models.

3.3 PLLaVA

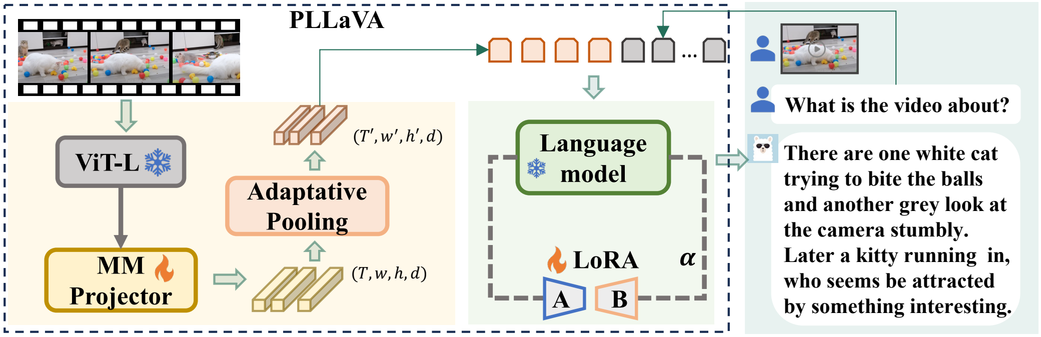

What is the video about?

There are one white cat trying to bite the balls and another grey look at the camera stumbly. Later a kitty running in, who seems be attracted by something interesting.

Figure 6: The framework of PLLaVA begins with processing a video from the user through ViT-L and MM projector, yielding visual features with shape (T, w, h, d). These features undergo Adaptive Pooling, which effectively reduces both temporal and spatial dimensions. The pooled features are then flattened and concatenated with question embeddings, serving as input to the image Large Language Model to generate response to the user. The weights of the image LLMs are fused with LoRA weight learned under video samples.

Motivation Our initial attempts on *n-frame* and VideoChatGPT [30] reveal the intricacies of adapting image-focused MLLMs to the video domain, encountering the data scaling problem. The former introduces a small amount of frames due to the limit of memory, whereas the latter compresses over 100 frames of information with pooling strategy. However, similar outcomes occur to both situations.

In view of the necessity of temporal information and the prohibited costs of dealing with very long video input to MLLMs, pooling is an intuitive and simple way to fulfill both of the requirements. The above two problems may stem from inadequacy of frame information and mishandling on the frame features. Therefore, in this paper, we deeply look into the pooling strategies for video features used in MLLMs.

Definition We formalize the pooling process for video features as follows, a model structure is shown in Figure 6. After feeding video frames $\mathbf{X} \in \mathbb{R}^{T \times C \times W \times H}$ into the CLIP-ViT model and the multimodal projector, we obtain an encoded vision feature $X_v \in \mathbb{R}^{T \times w \times h \times d}$ for a video input. This feature is then passed through a parameter-free Adaptive Structure Pooling module and reduced to a smaller size. Given the desired feature dimension $T' \times w' \times h'$, the process is formulated as:

$$X_{vp} = \text{AdaptStructPooling}(X_v | T' \times w' \times h'). \tag{2}$$

These features are then concatenated with text input embeddings and fed into the LLM to generate responses. We also include a LoRA [9] module to adapt the LLM to video-related generation tasks. In conclusion, the weights that will be updated are Multimodal Projector and LLM LoRA.

Within this framework, we investigated the impact of pooling through grid search analysis. Our findings suggest that pooling on the spatial dimension yields favorable outcomes, whereas temporal dimension pooling is associated with decreased performance. For a thorough exploration of our search process and the rationale behind this conclusion, please refer to Sec. 4.2.

3.4 Post Optimization

Regarding the problem of performance decline associated with scaled model size, such degradation may stem from diminished language proficiency resulting from training on low-quality video-text data samples. To mitigate this, we propose a post-training optimization approach for the parameters of the video MLLM. It involves blending the trained Language Model (LLM) on video data with the original LLM of the base image MLLM. For a pretrained MLLM with LLM parameters W_0 and given input X_{vp}, the output hidden states from the LoRA fine-tuned LLM can be acquired as follows:

$$h = W_0 X_{vp} + \frac{\alpha}{r} \Delta W X_{vp}, \tag{3}$$

where ΔW are a low-rank learnable parameters for adapting W_0, and $\frac{\alpha}{r}$ is used to scale the learned low-rank weight.

As part of our post-training optimization process, we tune the mix ratio between the original LLMs and the trained LLMs (incorporating LoRA weights) by varying the value of α during inference. Our experiments indicate that lower α yields significantly better generative performance.

4 Experiments

4.1 Experiment Setting

Data and Evaluation We leverage instructional video-to-text datasets to extend the capabilities of image MLLMs to handle video inputs. The training data are sourced from the VideoChat2 dataset [18], which embraces data for various video understanding tasks, including 27k for conversation combined from VideoChat [17] and Video-ChatGPT [30], 80k of classification from Kinetics [13] and SthSthV2 [6], 450k caption data from Webvid [2], YouCook2 [47], TextVR [37] and VideoChat, 117 reasoning data from NextQA [38] and CLEVRER [42] and 109K questioning answering data annotated from Webvid, TGIF [20] and Ego4D [7], totaling 783k instructional tuning data.

We evaluate our trained models with the following video-to-text benchmarks. First, the open-ended Video Question Answer (VideoQA) includes MSVD-QA [39], MSRVTT-QA [39], ActivityQA [43], and TGIF QA [20]. Responses in these question-answering benchmarks typically consist of single-word answers. GPT-3.5 is used to evaluate the accuracy (Accuracy, with answers true/false) and quality (Score, ranging from 0 to 5) of the models' responses. Additionally, we adopt the Video-based Generative Performance benchmark (referred to as VCG Score), introduced by VideoChatGPT [30]. These benchmarks often involve longer answers, encompassing five aspects of video understanding: CI (Correctness of Information), DO (Detail Orientation), CU (Context Understanding), TU (Temporal Understanding), and CO (Consistency). The generation is also assessed using the GPT-3.5 model. Furthermore, we also use the multi-choice Question Answering benchmark, MVBench [18], comprising 20 tasks that demand nuanced temporal comprehension of videos. This benchmark does not necessitate evaluation from the GPT-3.5 model.

Models and Implementation Details PLLaVA is constructed upon the image MLLMs, LLaVA Next [26, 25] models 7B, 13B, and 34B. We utilize their pre-trained weights available in the Hugging Face library[1] and integrate an adaptive pooling module to reduce feature dimensions before passing the input visual features to the LLM generation component. For the pooling layer, we uniformly select 16 frames as input and set the target pooling shape to be $16 \times 12 \times 12 \times d$, where d corresponds to the input dimension of the LLMs. During training, we employ a batch size of 128 and a learning rate of 2e-5, with a cosine scheduler and a warmup ratio of 0.03. All the reported results are evaluated on models trained for 6250 steps. For evaluation, we adopt the GPT-3.5-turbo-0125 model across all the benchmarks.

4.2 Impact of Pooling Operation Design

Considering the unsatisfying performance of the complete pooling on temporal and spatial dimensions adopted in Video-ChatGPT and the limitation information in the straightforward *n-frame* method, we further explore the influence of poling strategies here.

Pooling Layer Design Pooling can be done both temporally and spatially. In this part, we aim to figure out the answer to two questions: 1) which dimension is more suitable to be pooled to save the computational cost and 2) what is the largest compression ratio along that dimension. To achieve this, we plot a model curve based on the LLaVA-1.5 7B model with different temporal and spatial

[1] https://huggingface.co/docs/transformers/en/model_doc/llava_next

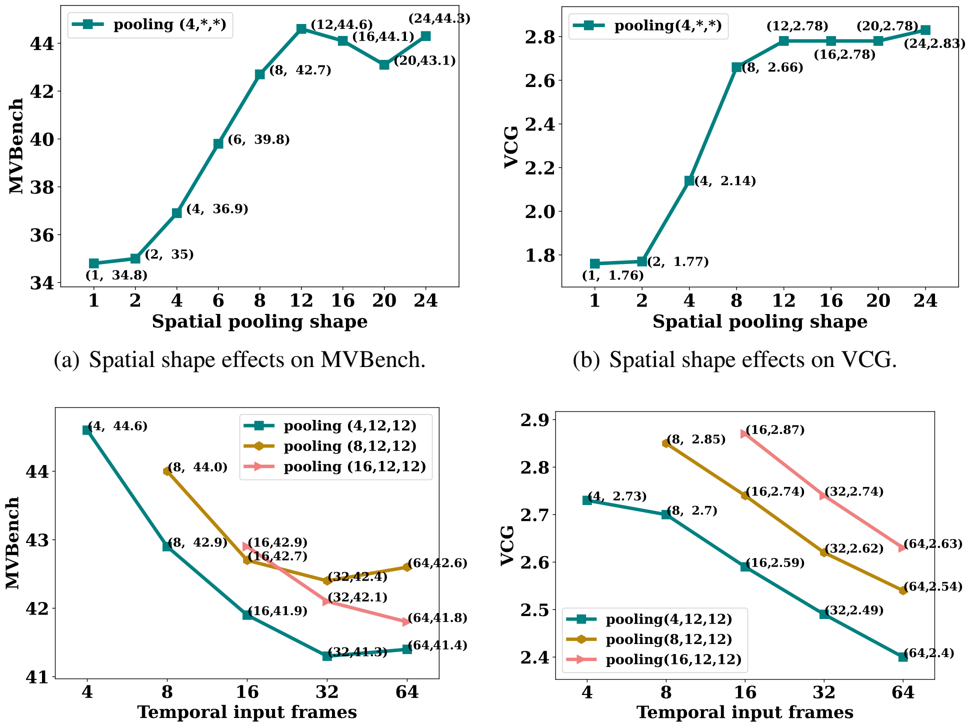

(a) Spatial shape effects on MVBench.

(b) Spatial shape effects on VCG.

(c) Temporal shape effects on MVBench.

(d) Temporal shape effects on VCG.

Figure 7: Pooling shape influence.

dimensions controlled via pooling operation. Specifically, for the spatial dimension, we picked an input video feature with shape (4,24,24,d), where 4 is the frame numbers (temporal dimension), 24×24 is the original spatial dimension of frame features, and d is the embedding dimension of each visual token. The target spatial shapes are chosen at evenly spaced intervals between 1 and 24, resulting in a set of spatial shapes $S = \{n \times n \mid n \in [1, 2, 4, 6, 8, 12, 16, 20, 24]\}$. The MVBench and VCG Score performance of these spatial pooling shapes are shown in Figure 7(a) and 7(b). It is observed that downsampling the spatial dimension by 50% does not degrade the model performance. Further reducing the spatial dimension would lead to a significant performance drop. Considering the tradeoff between computational overhead and performance, 12×12 can be a target spatial dimension.

We further experimented on the temporal dimension. Several target pooling shapes were chosen with spatial dimensions fixed as 12, including (4,12,12), (8,12,12), and (16,12,12). We study the pooling performance tendency when altering the number of input video frames, indicating the downsampling rate of poolings. For example, pooling from (64,24,24) to (4,12,12) indicates every 16 frames are fused, then the downsampling rate should be 6.25%. All of the resulting model curves are shown in Figure 7(c) and 7(d). Different from spatial pooling, the model performance is sensitive to the temporal pooling. As illustrated in these two figures, all lines achieve better performance with lower downsmapling rates. In other words, *pooling along temporal dimension always downgrades the model performance.*

Pooling Impact We found that pooling over more video frames not only improves the model efficiency but also makes the model more robust to user enquires. During our experiments, we evaluated models under different training iterations with two sets of prompts. For example, we vary the role tag from 'USER' to 'Human' during evaluation and the results are as shown in Figure 3. The figure shows that the visual feature norms learned with the pooling operation show consistent distributions under different training iterations compared to the 4-frame method that shows dominant tokens. This is also reflected in the model responses where the pooling method gives consistent good text responses while the 4-frames method gives shorter and shorter text responses as the training goes longer, or even no response when out-of-distribution prompts are used. This conclusion can be further validated by Figure 2. With pooling introduced, no matter what prompt is used or how much training sampled is learned, the text generation lengths with the pooling method are consistent. We owe the stability in generation to the smoothing ability of pooling, which eliminates the influence of dominant high norm tokens. For more rigorous analysis from the perspective of mathematical proofs, we leave it for future work.

4.3 Quatitative Results

Method	**Vision Encoder**	**LLM Size**	**MSVD-QA**		**MSRVTT-QA**		**ActivityNet-QA**		**TGIF-QA**		**Video-ChatGPT**					
			Acc.	**Sco.**	**Acc.**	**Sco.**	**Acc.**	**Sco.**	**Acc.**	**Sco.**	**CI**	**DO**	**CU**	**TU**	**CO**	**Avg.**
FrozenBiLM[40]	ViT-L	1.3B	33.8	-	16.7	-	25.9	-	41.9	-						
Video-LLaMA[45]	CLIP-G	7B	51.6	2.5	29.6	1.8	12.4	1.1	-	-	1.96	2.18	2.16	1.82	1.79	1.98
LLaMA-Adapter[46]	ViT-B	7B	54.9	3.1	43.8	2.7	34.2	2.7	-	-	2.03	2.32	2.30	1.98	2.15	2.16
Video-ChatGPT[30]	ViT-L	7B	64.9	3.3	49.3	2.8	35.2	2.7	51.4	3.0	2.50	2.57	2.69	2.16	2.20	2.42
Video-LLaVA[22]	ViT-L	7B	70.7	3.9	59.2	3.5	45.3	3.3	70.0	4.0						
Chat-UniVi[12]	ViT-L	7B	65.0	3.6	54.6	3.1	45.8	3.2	60.3	3.4	2.89	2.91	3.46	2.89	2.81	2.99
MovieChat[32]	CLIP-G	7B	75.2	3.8	52.7	2.6	45.7	3.4	-	-	2.76	2.93	3.01	2.24	2.42	2.67
VideoChat[17]	CLIP-G	7B	56.3	2.8	45.0	2.5	26.5	2.2	34.4	2.3	2.23	2.50	2.53	1.94	2.24	2.29
VideoChat2[18]	UMT-L	7B	70.0	3.9	54.1	3.3	49.1	3.3	-	-	3.02	2.88	3.51	2.66	2.81	2.98
Vista-LLaMA[29]	CLIP-G	7B	65.3	3.6	60.5	3.3	48.3	3.3	-	-	2.44	2.64	3.18	2.26	2.31	2.57
LLaMA-VID[19]	CLIP-G	13B	70.0	3.7	58.9	3.3	47.5	3.3	-	-	2.96	3.00	3.53	2.46	2.51	2.89
LITA [11]	CLIP-L	7B	-	-	-	-	-	-	-	-	2.94	2.98	3.43	2.68	3.19	3.04
ST-LLM [28]	BLIP2	7B	74.6	3.9	63.2	3.4	50.9	3.3	-	-	3.23	3.05	3.74	2.93	2.81	3.15
IG-VLM CogAgent[8]	CLIP-E	7B	76.7	4.1	62.7	3.6	57.3	3.6	76.7	4.0	3.26	2.76	3.57	2.34	3.28	3.04
IG-VLM LLaVA 7B [25]	ViT-L	7B	78.8	4.1	63.7	3.5	54.3	3.4	73.0	4.0	3.11	2.78	3.51	2.44	3.29	3.03
IG-VLM LLaVA 13B [25]	ViT-L	13B	77.4	4.1	62.6	3.4	57.1	3.5	78.0	4.0	3.17	2.79	3.52	2.51	3.25	3.05
IG-VLM LLaVA 34B [25]	ViT-L	34B	79.6	4.1	62.4	3.5	58.4	3.5	79.1	4.2	3.21	2.87	3.54	2.51	**3.34**	3.09
IG-VLM GPT-4V[1]	Unk	GPT-4	76.3	4.0	63.8	3.5	57.0	3.5	65.3	3.7	3.40	2.80	3.61	**2.89**	3.13	**3.17**
PLLaVA 7B	ViT-L	7B	76.6	4.1	62.0	3.5	56.3	3.5	77.5	4.1	3.21	2.86	3.62	2.33	2.93	3.12
PLLaVA 13B	ViT-L	13B	75.7	4.1	63.2	3.6	56.3	3.6	77.8	4.2	3.27	2.99	3.66	2.47	3.09	3.27
PLLaVA 34B	ViT-L	34B	**79.9**	**4.2**	**68.7**	**3.8**	**60.9**	**3.7**	**80.6**	**4.3**	**3.60**	**3.20**	**3.90**	2.67	3.25	**3.48**
Improve over GPT-4V [14]	-	-	+3.6	+0.2	4.9	0.3	3.9	0.2	15.3	0.6	0.2	0.4	0.3	-0.32	0.12	0.31

Table 2: Results of video question-answering.

Table 2 demonstrates the results on VideoQA. PLLaVA 34B significantly outperforms all the existing methods on the Accuracy and Score metrics of MSVD, MSRVTT, ActivityNet, and TGIF. Compared to GPT-4V, PLLaVA 34B achieves improvement margins of 3.6, 4.9, 3.9, and 15.3 on these four benchmarks. The performance of PLLaVA with 7B and 13B model sizes also exceeds all the baselines on the Score metric. These results not only prove the capability of our model in conducting video question answering but also highlight the superiority of our pooling strategy in scaling model size.

PLLaVA also achieved a new state-of-the-art in the average VCG score. The 7B, 13B, and 34B versions have all outperformed their best counterparts of the same LLM size, with margins of 2.9%, 7.1%, and 12.6%, respectively. Notably, PLLaVA achieves superior performance on CI(correctness of information), DO(Detail Orientation), and CU(Context Understanding) compared to the previous SOTA, with 34B exceeding them by 5.8%, 6.7%, 9.2%. These results indicate that PLLaVA will be of great potential to do detailed video captioning. As for TU(temporal understanding), PLLaVA 34B exceeds its fair opponent IG-VLM LLaVA 34B by 6%. Compared with models that utilize the specialized video encoder, VideoChat2, or a more complicated frame combination method, Chat-Univ, PLLaVA still has some room for improvement by fingering the pooling strategy or incorporating a better vision encoder. CO(Consistency) measures generation consistency when the model encounters different questions that lead to similar answers. Compared to baselines except for IG-VLM, our model achieves much better consistency.

MVBench is a comprehensive video understanding benchmark, focusing on questions that require overall comprehension of multiple frames. As shown in Table 3, PLLaVA surpasses the previous SOTA VideoChat2 with a margin of 13.7% on average across 20 tasks. If we look into each aspect of MVBench, our method performs very well, concerning 17 out of 20 tasks of MVBench, which shows that our model has the superiority to understand many fine-grained details about videos accurately. However, we also noticed some aspects of our model still need to improve, such as CI(CounterFactual Inference) and OS(object shuffle). CI is used to predict what might happen if an event occurs, and OS is used to locate the final position of an object in an occlusion game. These two require strong reasoning ability and imagination to answer. VideoChat2 is pretrained with a large amount of video data with a specialized video encoder and fine-tuned with both video and image reasoning data, thus presenting better performance in these aspects.

Method	Vision Encoder	LLM Size	AS	AP	AA	FA	UA	OE	OI	OS	MD	AL	ST	AC	MC	MA	SC	FP	CO	EN	ER	CI	Avg.
Video-LLaMA [45]	CLIP-G	7B	27.5	25.5	51.0	29.0	39.0	48.0	40.5	38.0	22.5	22.5	43.0	34.0	22.5	32.5	45.5	32.5	40.0	30.0	21.0	37.0	34.1
LLaMA-Adapter [46]	ViT-B	7B	23.0	28.0	51.0	30.0	33.0	53.5	32.5	33.5	25.5	21.5	30.5	29.0	22.5	41.5	39.5	25.0	31.5	22.5	28.0	32.0	31.7
Video-ChatGPT [30]	ViT-L	7B	23.5	26.0	62.0	22.5	26.5	54.0	28.0	40.0	23.0	20.0	31.0	30.5	25.5	39.5	48.5	29.0	33.0	29.5	26.0	35.5	32.7
VideoChat [17]	CLIP-G	7B	33.5	26.5	56.0	33.5	40.5	53.0	40.5	30.0	25.5	27.0	48.5	35.0	20.5	42.5	46.0	26.5	41.0	23.5	23.5	36.0	35.5
VideoChat2 [18]	UMT-L	7B	66.0	47.5	**83.5**	**49.5**	60.0	58.0	**71.5**	**42.5**	23.0	23.0	88.5	39.0	42.0	58.5	44.0	49.0	36.5	35.0	40.5	**65.5**	51.1
ST-LLM [28]	BLIP2	7B	66.0	53.5	84.0	44.0	58.5	80.5	73.5	38.5	42.5	31.0	86.5	36.5	56.5	78.5	43.0	44.5	46.5	34.5	41.5	58.5	54.9
GPT-4V	Unk	GPT-4	55.5	**63.5**	72.0	46.5	73.5	18.5	59.0	29.5	12.0	40.5	83.5	39.0	12.0	22.5	45.0	47.5	52.0	31.0	59.0	11.0	43.5
PLLaVA 7B	ViT-L	7B	58.0	49.0	55.5	41.0	61.0	56.0	61.0	36.0	23.5	26.0	82.0	39.5	42.0	52.0	45.0	42.0	53.5	30.5	48.0	31.0	46.6
PLLaVA 13B	ViT-L	13B	66.0	53.0	65.5	45.0	65.0	58.0	64.5	35.5	23.5	30.0	85.0	39.5	45.5	57.0	47.5	49.5	49.0	33.0	53.0	37.0	50.1
PLLaVA 34B	ViT-L	34B	**67.5**	53.0	82.0	47.0	**79.0**	**68.5**	67.5	36.5	**37.5**	**49.5**	**91.0**	**40.5**	**43.0**	**70.0**	**51.5**	**50.0**	**66.5**	**39.5**	**63.5**	59.0	**58.1**
Improve over GPT-4V	-	-	12.0	-10.5	10.0	1.5	5.5	50	8.5	7.0	25.5	9.0	7.5	1.5	31.0	57.5	5.5	2.5	14.5	8.5	4.5	48.0	14.5

Table 3: Results on MVBench multi-choice question answering.

4.4 Analysis

Our PLLaVA is a simple and parameter-efficient method to adapt image MLLMs into the video domain. We also provide a feasible way to scale the models to larger sizes, which we found is hard to achieve in other methods such as ChatUniv [12] and IG-VLM [14]. In the following, we further provide some analysis related to the explanations on pooling shapes and the influence of LoRA weight on different tasks.

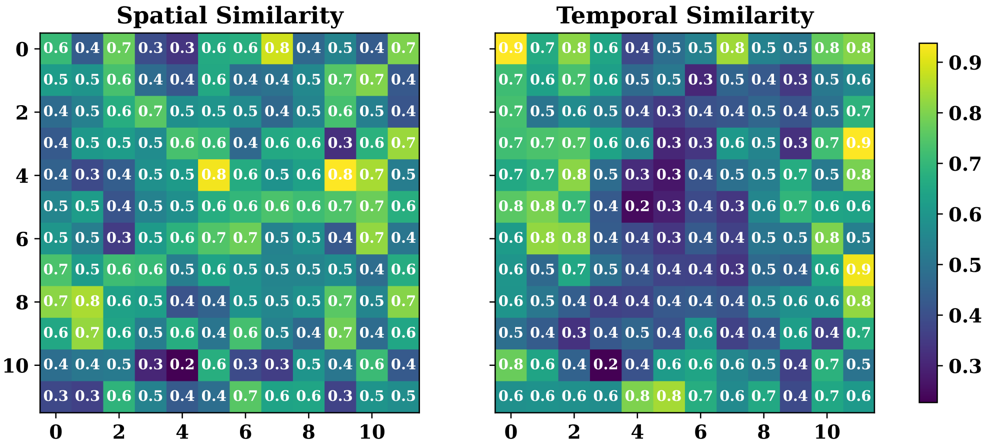

Figure 8: Vision token embedding similarities between spatial token neighbors and temporal token neighbors.

Temporal or spatial pooling? In Sec.4.2, we have illustrated the impact of temporal and spatial poolings, concluding that pooling along the temporal dimension consistently results in decreased performance compared to retaining the original frame numbers. We attribute this phenomenon to the interference with token features. In image MLLMs, features are derived from images/video frames using CLiP-ViT models, which produce embedded patches for each image/video frame, resulting in a video feature with shape (T, H, W). Pooling changes the dimensions of T (time), H (height), and W (weight). In contrast to pooling along the spatial dimension (local pooling on single images/frames, changing H and W), pooling along the temporal dimension (changing T) risks altering the original frame features. To validate the guess, we visualize token similarities among spatial and temporal token neighbors for a video feature in Figure 8. The two subfigures reveal significantly higher similarities within spatial neighbors than temporal neighbors. This observation supports the potential distortion of original token features caused by temporal pooling. LLMs are designed for sequence understanding. Even without preprocessing on temporal information aggregation, they can model temporal relations.

Image? Video? or Both? Post-training optimization is defined as the combination of the LLMs' parameters of image MLLMs and learned LLMs' LoRA weights from video samples. A suitable fusion ratio could be highly efficient in boosting model performance trained under low-quality video-text samples. Here, we discuss the influence of different choices of fusion ratio on the understanding performance. As shown in Figure 9, the x-axis represents the alpha value of LoRA.

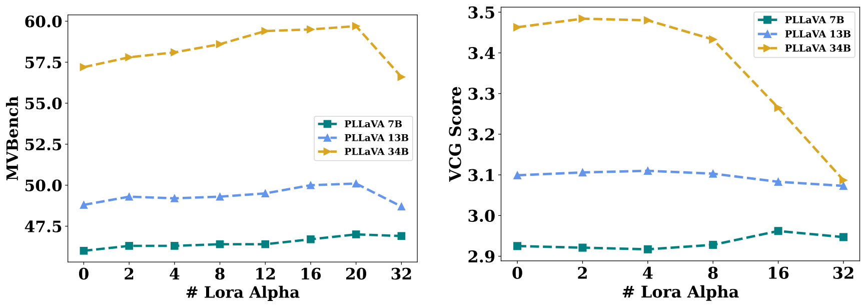

(a)

(b)

Figure 9: Influence of downsampling rate on MVBench(a) and VCG Score(b) performance. x-axis indicate the

0 indicates no LoRA weights added, and 32 means the LoRA weights are fully applied to LLMs. We observed distinct trends between MVBench and VCG Score. The former exhibits a peak around alpha 20, while the latter performs best near alpha 4. This variance can be attributed to the nature of these two benchmarks: VCG typically involves longer length generations, whereas MVBench focuses on multiple-choice question answering, placing less emphasis on language generation ability. Consequently, weights learned from video-text data samples are more tailored for MVBench tasks. In this way, a larger portion of video weights are beneficial for MVBench. Moreover, from these two figures, it's evident that combining video and image weights leads to better performance than at the extremes of 0 and 32.

4.5 Case Studies

Apart from these quantitative results, we also qualitatively investigate the video understanding abilities of PLLaVA models. We have shown several caption examples in Figure 10. According to the video clips, compared to IG-VLM, PLLaVA 34B recognizes more details about videos, including the clothes worn by the main characters, the environment, and even some of the words in this video. Besides, as shown in Figure 10(b), PLLaVA can understand the video content more correctly, in which people are playing badminton rather than volleyball. These mistakes made by IG-VLM could be caused by the lowered resolution when concatenating frames into the grid view in the method design. Pooling reduces dimension after frames are encoded, thus leading to less information loss.

4.6 Dense Recaption

In view of the caption ability of PLLaVA , we further tested its recaption task and contributed 1K video Inter4K [33] caption dataset. An example is shown in Figure 11. Compared to Open-Sora GPT-4 pipeline, our model captures better caption details and also highlights motion information in the video, demonstrate PLLaVA 's potential to contribute to the video generation community.

5 Conclusion

In this paper, we conduct an initial investigation for extending image-language models to videos with a simple yet extremely effective method, termed PLLaVA . With the new model, it is easier to scale the training with more data and larger large language models with a more controllable strategy for over-training and performance saturation. PLLaVA 's ability of giving detailed captions also contributes to the community development of multimodal understanding and generation.

What happens in the video?

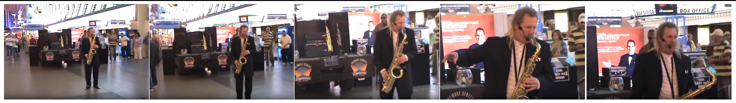

IG-VLM 34b: a man is playing a saxophone in various indoor settings, likely a shopping mall or a public space, with different lighting and background elements.

PLAVA 34b: In the video, there is a man playing a saxophone in what appears to be a public space, possibly a mall or a street. He is dressed in a suit and tie, which suggests that he might be a professional musician performing for an audience. There are other people in the background, indicating that this is a public area with some foot traffic. The setting looks like it could be a shopping center or a similar venue where live music is sometimes performed to entertain visitors.

(a) Badminton match.

What happens in the video?

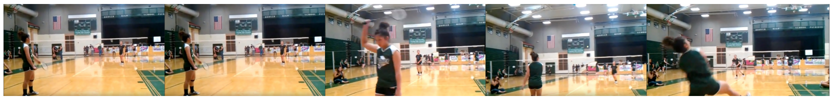

IGVLM: a group of people are playing a game of volleyball in an indoor gymnasium. The keyframes show various stages of the game, including players serving, hitting, and defending the ball. The gym is equipped with multiple nets and has a large audience watching the game.

PLAVA: The video shows an indoor gymnasium where a group of people are playing badminton. There are multiple badminton courts set up, and players are engaged in matches. The gymnasium has a high ceiling with fluorescent lighting, and there are banners and signs on the walls, including one that reads "HOOVER HIGH." The players are wearing athletic attire suitable for badminton, and they are using badminton rackets to hit shuttlecocks back and forth across the net

(b) Street Saxophone.

Figure 10: Case Studies.

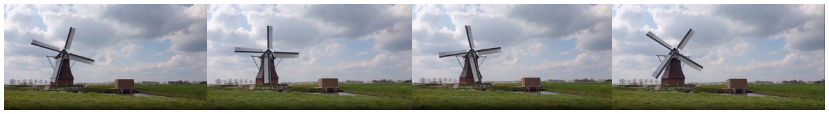

PLLaVA 34B

The video shows a large, traditional Dutch windmill situated on a grassy area next to a body of water, possibly a river or a canal. The windmill has a prominent presence in the scene, with its sails visible and appearing to be in motion. In the background, there is a small building, which could be a storage shed or a house, and a fence. The sky is partly cloudy, suggesting a changeable weather condition. There are no characters or actions visible in the video, as it is a static scene with no people or animals present. The focus of the video is on the windmill and its surroundings, providing a glimpse into the traditional landscape of the Netherlands.

Open-Sora GPT-4 Caption Pipeline

OPEN SORA

The video showcases a traditional Dutch windmill set against a partially cloudy sky, with a gently flowing waterway in the foreground. Surrounding the windmill is a lush green field dotted with yellow wildflowers. A small outbuilding is adjacent to the windmill, separated by a quaint wooden fence. The peaceful rural landscape suggests the tranquil pace of life in the count side, with the windmill standing as an iconic symbol of Dutch heritage. The windmill's sails are stationary, implying a calm day without much wind.

Figure 11: Recaption comparison between PLLaVA 34B and Open-Sora.

References

[1] Josh Achiam, Steven Adler, Sandhini Agarwal, Lama Ahmad, Ilge Akkaya, Florencia Leoni Aleman, Diogo Almeida, Janko Altenschmidt, Sam Altman, Shyamal Anadkat, et al. Gpt-4 technical report. *arXiv preprint arXiv:2303.08774*, 2023.

[2] Max Bain, Arsha Nagrani, Gül Varol, and Andrew Zisserman. Frozen in time: A joint video and image encoder for end-to-end retrieval. In *Proceedings of the IEEE/CVF International Conference on Computer Vision*, pages 1728–1738, 2021.

[3] Guo Chen, Yin-Dong Zheng, Jiahao Wang, Jilan Xu, Yifei Huang, Junting Pan, Yi Wang, Yali Wang, Yu Qiao, Tong Lu, et al. Videollm: Modeling video sequence with large language models. *arXiv preprint arXiv:2305.13292*, 2023.

[4] Mark Chen, Jerry Tworek, Heewoo Jun, Qiming Yuan, Henrique Ponde de Oliveira Pinto, Jared Kaplan, Harri Edwards, Yuri Burda, Nicholas Joseph, Greg Brockman, et al. Evaluating large language models trained on code. *arXiv preprint arXiv:2107.03374*, 2021.

[5] Rohan Choudhury, Koichiro Niinuma, Kris M. Kitani, and László A. Jeni. Zero-shot video question answering with procedural programs. *ArXiv abs/2312.00937*, 2023.

[6] Raghav Goyal, Samira Ebrahimi Kahou, Vincent Michalski, Joanna Materzynska, Susanne Westphal, Heuna Kim, Valentin Haenel, Ingo Fruend, Peter Yianilos, Moritz Mueller-Freitag, et al. The" something something" video database for learning and evaluating visual common sense. In *Proceedings of the IEEE international conference on computer vision*, pages 5842–5850, 2017.

[7] Kristen Grauman, Andrew Westbury, Eugene Byrne, Zachary Chavis, Antonino Furnari, Rohit Girdhar, Jackson Hamburger, Hao Jiang, Miao Liu, and Xingyu Liu et al. Ego4d: Around the world in 3,000 hours of egocentric video. *IEEE Conf. Comput. Vis. Pattern Recog.*, pages 18995–19012, 2022.

[8] Wenyi Hong, Weihan Wang, Qingsong Lv, Jiazheng Xu, Wenmeng Yu, Junhui Ji, Yan Wang, Zihan Wang, Yuxuan Zhang, Juanzi Li, Bin Xu, Yuxiao Dong, Ming Ding, and Jie Tang. Cogagent: A visual language model for gui agents. *ArXiv*, abs/2312.08914, 2023.

[9] Edward J Hu, Phillip Wallis, Zeyuan Allen-Zhu, Yuanzhi Li, Shean Wang, Lu Wang, Weizhu Chen, et al. Lora: Low-rank adaptation of large language models. In *International Conference on Learning Representations*, 2021.

[10] Bin Huang, Xin Wang, Hong Chen, Zihan Song, and Wenwu Zhu. Vtimellm: Empower llm to grasp video moments, 2023.

[11] De-An Huang, Shijia Liao, Subhashree Radhakrishnan, Hongxu Yin, Pavlo Molchanov, Zhiding Yu, and Jan Kautz. Lita: Language instructed temporal-localization assistant. *arXiv preprint arXiv:2403.19046*, 2024.

[12] Peng Jin, Ryuichi Takanobu, Caiwan Zhang, Xiaochun Cao, and Li Yuan. Chat-univi: Unified visual representation empowers large language models with image and video understanding. *ArXiv abs/2311.08046*, 2024.

[13] Will Kay, Joao Carreira, Karen Simonyan, Brian Zhang, Chloe Hillier, Sudheendra Vijayanarasimhan, Fabio Viola, Tim Green, Trevor Back, Paul Natsev, et al. The kinetics human action video dataset. *arXiv preprint arXiv:1705.06950*, 2017.

[14] Wonkyun Kim, Changin Choi, Wonseok Lee, and Wonjong Rhee. An image grid can be worth a video: Zero-shot video question answering using a vlm. *arXiv preprint arXiv:2403.18406*, 2024.

[15] Yann LeCun, Bernhard Boser, John Denker, Donnie Henderson, Richard Howard, Wayne Hubbard, and Lawrence Jackel. Handwritten digit recognition with a back-propagation network. *Advances in neural information processing systems*, 2, 1989.

[16] Junnan Li, Dongxu Li, Silvio Savarese, and Steven Hoi. Blip-2: Bootstrapping language-image pre-training with frozen image encoders and large language models. In *International conference on machine learning*, pages 19730–19742. PMLR, 2023.

[17] KunChang Li, Yinan He, Yi Wang, Yizhuo Li, Wenhai Wang, Ping Luo, Yali Wang, Limin Wang, and Yu Qiao. Videochat: Chat-centric video understanding. *arXiv preprint arXiv:2305.06355*, 2023.

[18] Kunchang Li, Yali Wang, Yinan He, Yizhuo Li, Yi Wang, Yi Liu, Zun Wang, Jilan Xu, Guo Chen, Ping Luo, et al. Mvbench: A comprehensive multi-modal video understanding benchmark. *ArXiv abs/2311.17005*, 2023.

[19] Yanwei Li, Chengyao Wang, and Jiaya Jia. Llama-vid: An image is worth 2 tokens in large language models. *ArXiv abs/2311.17043*, 2023.

[20] Yuncheng Li, Yale Song, Liangliang Cao, Joel Tetreault, Larry Goldberg, Alejandro Jaimes, and Jiebo Luo. Tgif: A new dataset and benchmark on animated gif description. In *Proceedings of the IEEE Conference on Computer Vision and Pattern Recognition*, pages 4641–4650, 2016.

[21] Long Lian, Boyi Li, Adam Yala, and Trevor Darrell. Llm-grounded diffusion: Enhancing prompt understanding of text-to-image diffusion models with large language models. *arXiv preprint arXiv:2305.13655*, 2023.

[22] Bin Lin, Bin Zhu, Yang Ye, Munan Ning, Peng Jin, and Li Yuan. Video-llava: Learning united visual representation by alignment before projection. *ArXiv abs/2311.10122*, 2023.

[23] Ji Lin, Hongxu Yin, Wei Ping, Yao Lu, Pavlo Molchanov, Andrew Tao, Huizi Mao, Jan Kautz, Mohammad Shoeybi, and Song Han. Vila: On pre-training for visual language models. *arXiv preprint arXiv:2312.07533*, 2023.

[24] Haotian Liu, Chunyuan Li, Yuheng Li, and Yong Jae Lee. Improved baselines with visual instruction tuning. In *NeurIPS 2023 Workshop on Instruction Tuning and Instruction Following*, 2023.

[25] Haotian Liu, Chunyuan Li, Yuheng Li, Bo Li, Yuanhan Zhang, Sheng Shen, and Yong Jae Lee. Llava-next: Improved reasoning, ocr, and world knowledge, January 2024.

[26] Haotian Liu, Chunyuan Li, Qingyang Wu, and Yong Jae Lee. Visual instruction tuning. *Advances in neural information processing systems*, 36, 2024.

[27] Ruyang Liu, Chen Li, Yixiao Ge, Ying Shan, Thomas H Li, and Ge Li. One for all: Video conversation is feasible without video instruction tuning. *arXiv preprint arXiv:2309.15785*, 2023.

[28] Ruyang Liu, Chen Li, Haoran Tang, Yixiao Ge, Ying Shan, and Ge Li. St-llm: Large language models are effective temporal learners. *arXiv preprint arXiv:2404.00308*, 2024.

[29] Fan Ma, Xiaojie Jin, Heng Wang, Yuchen Xian, Jiashi Feng, and Yi Yang. Vista-llama: Reliable video narrator via equal distance to visual tokens. *ArXiv abs/2312.08870*, 2023.

[30] Muhammad Maaz, Hanoona Rasheed, Salman Khan, and Fahad Shahbaz Khan. Video-chatgpt: Towards detailed video understanding via large vision and language models. *arXiv preprint arXiv:2306.05424*, 2023.

[31] Alec Radford, Jong Wook Kim, Chris Hallacy, Aditya Ramesh, Gabriel Goh, Sandhini Agarwal, Girish Sastry, Amanda Askell, Pamela Mishkin, Jack Clark, et al. Learning transferable visual models from natural language supervision. In *International conference on machine learning*, pages 8748–8763. PMLR, 2021.

[32] Enxin Song, Wenhao Chai, Guanhong Wang, Yucheng Zhang, Haoyang Zhou, Feiyang Wu, Xun Guo, Tianbo Ye, Yang Lu, Jenq-Neng Hwang, and Gaoang Wang. Moviechat: From dense token to sparse memory for long video understanding. *ArXiv abs/2307.16449*, 2023.

[33] Alexandros Stergiou and Ronald Poppe. Adapool: Exponential adaptive pooling for information-retaining downsampling. *IEEE Transactions on Image Processing*, 32:251–266, 2022.

[34] Dídac Surís, Sachit Menon, and Carl Vondrick. Vipergpt: Visual inference via python execution for reasoning. *Proceedings of IEEE International Conference on Computer Vision (ICCV)*, 2023.

[35] Hugo Touvron, Thibaut Lavril, Gautier Izacard, Xavier Martinet, Marie-Anne Lachaux, Timothée Lacroix, Baptiste Rozière, Naman Goyal, Eric Hambro, Faisal Azhar, et al. Llama: Open and efficient foundation language models. *arXiv preprint arXiv:2302.13971*, 2023.

[36] Ashish Vaswani, Noam Shazeer, Niki Parmar, Jakob Uszkoreit, Llion Jones, Aidan N Gomez, Łukasz Kaiser, and Illia Polosukhin. Attention is all you need. *Advances in neural information processing systems*, 30, 2017.

[37] Weijia Wu, Yuzhong Zhao, Zhuang Li, Jiahong Li, Hong Zhou, Mike Zheng Shou, and Xiang Bai. A large cross-modal video retrieval dataset with reading comprehension. *arXiv preprint arXiv:2305.03347*, 2023.

[38] Junbin Xiao, Xindi Shang, Angela Yao, and Tat-Seng Chua. Next-qa: Next phase of question-answering to explaining temporal actions. In *Proceedings of the IEEE/CVF conference on computer vision and pattern recognition*, pages 9777–9786, 2021.

[39] Dejing Xu, Zhou Zhao, Jun Xiao, Fei Wu, Hanwang Zhang, Xiangnan He, and Yueting Zhuang. Video question answering via gradually refined attention over appearance and motion. In *Proceedings of the 25th ACM international conference on Multimedia*, pages 1645–1653, 2017.

[40] Antoine Yang, Antoine Miech, Josef Sivic, Ivan Laptev, and Cordelia Schmid. Zero-shot video question answering via frozen bidirectional language models. *Adv. Neural Inform. Process. Syst.*, 35:124–141, 2022.

[41] Qilang Ye, Zitong Yu, Rui Shao, Xinyu Xie, Philip Torr, and Xiaochun Cao. Cat: Enhancing multimodal large language model to answer questions in dynamic audio-visual scenarios. *arXiv preprint arXiv:2403.04640*, 2024.

[42] Kexin Yi, Chuang Gan, Yunzhu Li, Pushmeet Kohli, Jiajun Wu, Antonio Torralba, and Joshua B Tenenbaum. Clevrer: Collision events for video representation and reasoning. In *International Conference on Learning Representations*, 2020.

[43] Zhou Yu, Dejing Xu, Jun Yu, Ting Yu, Zhou Zhao, Yueting Zhuang, and Dacheng Tao. Activitynet-qa: A dataset for understanding complex web videos via question answering. In *AAAI*, pages 9127–9134, 2019.

[44] Ce Zhang, Taixi Lu, Md Mohaiminul Islam, Ziyang Wang, Shoubin Yu, Mohit Bansal, and Gedas Bertasius. A simple llm framework for long-range video question-answering. *ArXiv abs/2312.17235*, 2023.

[45] Hang Zhang, Xin Li, and Lidong Bing. Video-LLaMA: An instruction-tuned audio-visual language model for video understanding. In *Conf. Empirical Methods in Natural Language Processing*, pages 543–553, 2023.

[46] Renrui Zhang, Jiaming Han, Aojun Zhou, Xiangfei Hu, Shilin Yan, Pan Lu, Hongsheng Li, Peng Gao, and Yu Qiao. Llama-adapter: Efficient fine-tuning of language models with zero-init attention. *arXiv preprint arXiv:2303.16199*, 2023.

[47] Luowei Zhou, Chenliang Xu, and Jason Corso. Towards automatic learning of procedures from web instructional videos. In *Proceedings of the AAAI Conference on Artificial Intelligence*, 2018.

[48] Deyao Zhu, Jun Chen, Xiaoqian Shen, Xiang Li, and Mohamed Elhoseiny. Minigpt-4: Enhancing vision-language understanding with advanced large language models. In *The Twelfth International Conference on Learning Representations*, 2023.